2016

Detection of Electrical Alternans in Ventricular Depolarization Phase of Human Electrocardiogram

David R. Wasemiller
University of Kentucky, david.wasemiller@uky.edu
Digital Object Identifier: https://doi.org/10.13023/ETD.2017.002

STUDENT AGREEMENT:

I represent that my thesis or dissertation and abstract are my original work. Proper attribution has been given to all outside sources. I understand that I am solely responsible for obtaining any needed copyright permissions. I have obtained needed written permission statement(s) from the owner(s) of each third-party copyrighted matter to be included in my work, allowing electronic distribution (if such use is not permitted by the fair use doctrine) which will be submitted to UKnowledge as Additional File.

I hereby grant to The University of Kentucky and its agents the irrevocable, non-exclusive, and royalty-free license to archive and make accessible my work in whole or in part in all forms of media, now or hereafter known. I agree that the document mentioned above may be made available immediately for worldwide access unless an embargo applies.

I retain all other ownership rights to the copyright of my work. I also retain the right to use in future works (such as articles or books) all or part of my work. I understand that I am free to register the copyright to my work.

REVIEW, APPROVAL AND ACCEPTANCE

The document mentioned above has been reviewed and accepted by the student's advisor, on behalf of the advisory committee, and by the Director of Graduate Studies (DGS), on behalf of the program; we verify that this is the final, approved version of the student's thesis including all changes required by the advisory committee. The undersigned agree to abide by the statements above.

David R. Wasemiller, Student

Dr. Abhijit Patwardhan, Major Professor

Dr. Abhijit Patwardhan, Director of Graduate Studies

DETECTION OF ELECTRICAL ALTERNANS IN VENTRICULAR DEPOLARIZATION PHASE OF HUMAN ELECTROCARDIOGRAM.

THESIS

A thesis submitted in partial fulfillment of the
requirements for the degree of Master of Science in
Biomedical Engineering in the College of Engineering
at the University of Kentucky

By

David Wasemiller

Lexington, Kentucky

Director: Dr. Abhijit Patwardhan, Professor of Biomedical Engineering

Lexington, Kentucky

2016

ABSTRACT OF THESIS

DETECTION OF ELECTRICAL ALTERNANS IN VENTRICULAR DEPOLARIZATION PHASE OF HUMAN ELECTROCARDIOGRAM.

T-wave Alternans (TWA) in an electrocardiogram (ECG) has received considerable interest as a potential predictor of sudden cardiac death (SCD). However, large clinical trials have shown that while TWA has a very high negative predictive value, its positive predictive value is poor. Results of previous studies suggest that arrhythmia onset can be affected by the phase relationship of alternans of the depolarization and repolarization phase of the action potentials of the ventricles. To assess this relationship, one would first need to establish that depolarization alternans can be detected and then develop methods to determine its relationship with repolarization alternans, which is TWA. The objective of this thesis was to determine whether depolarization phase alternans can be detected in clinical grade ECGs. To accomplish this, an algorithm was developed to quantify R-Wave alternans (RWA) in patients who display TWA in their ECGs. Using both the morphology and amplitude of the R-wave, our results show that RWA can be seen in clinical ECGs. This suggests that RWA has the potential to help quantify occurrence and incidence of depolarization alternans, and supports further exploration of the link between depolarization and repolarization alternans which has the potential to improve clinical utility of TWA.

KEYWORDS: Depolarization, Repolarization, Alternans, Electrocardiogram, TWA

David Wasemiller

12/20/2016

DETECTION OF ELECTRICAL ALTERNANS IN VENTRICULAR DEPOLARIZATION PHASE OF HUMAN ELECTROCARDIOGRAM.

By

David Ray Wasemiller

Dr. Abhijit Patwardhan
Director of Thesis

Dr. Abhijit Patwardhan
Director of Graduate Studies

12/20/2016
Date

This thesis work is dedicated to my wife, Beth-Anne, who has always stood by my side during the challenges of graduate school and life. I am truly thankful for having you in my life. This work is also dedicated to my daughter, Lauryn, who has brought so much joy to my life. I am very blessed to have you as a daughter.

Acknowledgments

I would like to acknowledge my advisor Dr. Abhijit Patwardhan, for his advice, encouragement and continual assistance

Table of Contents

List of Tables

List of Figures

List of Equations

Chapter 1 Introduction

Sudden Cardiac Death (SCD) is a condition where unexpected natural death, from cardiac causes, occurs within a short period of time from the initial onset of symptoms [1]. It accounts for over 300,000 deaths in the United States each year [2, 3]. With the onset of death occurring quickly after the first symptom, research has looked for ways to predict if someone is at risk for SCD. One particular abnormality that has received attention in the past 30 years, is the detection of T-Wave Alternans (TWA) in an electrocardiogram (ECG) during a standard stress test [4]. TWA is a result of the action potential (AP) duration (APD) alternating in length from beat-to-beat during the repolarization phase. This phenomenon has been linked to electrical instability within in the heart and can contribute to ventricular arrhythmias.

A recent meta-data study looked at over 2,600 subjects from 19 different studies and found that even though TWA test has a strong negative predictive value (NPV) (97.2%), its positive predictive value (PPV) (19.3%) is very weak [5]. This means that if the test is negative, the patient is unlikely to experience SCD within the next two years. Whereas if the test is positive, the patient's certainty of having SCD in the next two years is unknown. This can result in unnecessary treatment, potentially costing the patient money, time, and unnecessary anxiety.

One area of study that shows promise in improving the PPV of the TWA test is the relationship between alternans in the depolarization and repolarization phases of APs. A study from our laboratory reported in 2012 that when APD alternans was present in cardiac tissue, alternans in the max rate of repolarization ($|dv/dt|_{max}$) was also present but the two were not always in phase [6]. Taking this knowledge and using a canine ventricular myocyte mathematical model, they investigated the effects of the phase between APD and $|dv/dt|_{max}$ alternans. In the model, if the two alternans were in-phase, the alternans of the cells became discordant, which is a phenomenon where short (long) activation of short-long sequence becomes long (short) as it travels spatially. However, if they were out-of-phase, no discord occurred. Indicating that when the APD and $|dv/dt|_{max}$ alternans are out-of-phase, it might have a stabilizing effect and affect discord incidence.

In looking for a marker that could be used to identify the presence of $|dv/dt|_{max}$ alternans in ECG, a dipole field potential spatial model was used (unpublished results by Drs. A.R Patwardhan and S. Wang). The results of the simulations showed that alternans of $|dv/dt|_{max}$ resulted in alternans of the R wave amplitude. The purpose of the present thesis is to determine whether beat-to-beat changes in morphology of the R-Wave are seen in clinical grade ECGs when TWA is also present. The results of prior studies from our group suggest that if such changes did occur, inclusion of these in future studies has the potential to improve the diagnostic value of TWA for SCD.

Chapter 2 Background

2.1 Cardiac Cycle

The main function of the heart is to pump blood throughout the body. The human heart is divided into two sides. The right side is responsible for collecting the oxygen-depleted blood from the body and sending it to the lungs. The left side is responsible for receiving oxygen rich blood from the lungs and pumping it throughout the body. Each side of the heart has two chambers, the upper chamber, called the atria, and the lower chamber, called the ventricle.

The cardiac cycle consists of two stages. First the diastole stage, where the heart is relaxed and the atria are filling with blood. Next, in the systole stage, the heart contracts in an organized manner to pump blood from ventricles out of the heart. The sinoatrial (SA) node located in the upper part of the right atrium controls this cycle. At the start of the systole stage, an AP is generated by a SA node, and propagated throughout both atria. This causes the atria to constrict, increasing pressure and pushing blood into the ventricles. Once the AP reaches the atrioventricular (AV) node, it is delayed shortly before continuing on to the ventricles. The AV node is a group of pacemaker cells located between the atrium and ventricles that allows the AP to pass through an otherwise electrically insulated wall. This short delay gives the atrium enough time to finish pumping blood into the ventricles and helps to prevent atrial arrhythmias from spreading to the ventricles. After the short delay, the AP continues down the Bundle of His to the left and right ventricle through the Purkinje fibers, for a rapid constriction of the ventricles, pushing blood out of the heart.

2.2 Cardiac Action Potential

A cardiac AP is a brief change in transmembrane potential (TMP) of muscle cells within the heart. This change is typically caused by the opening and closing of specific ion channels that cross a cell’s membrane. The cardiac AP consists of 5 phases typically labeled 0-4, beginning and ending with phase 4.

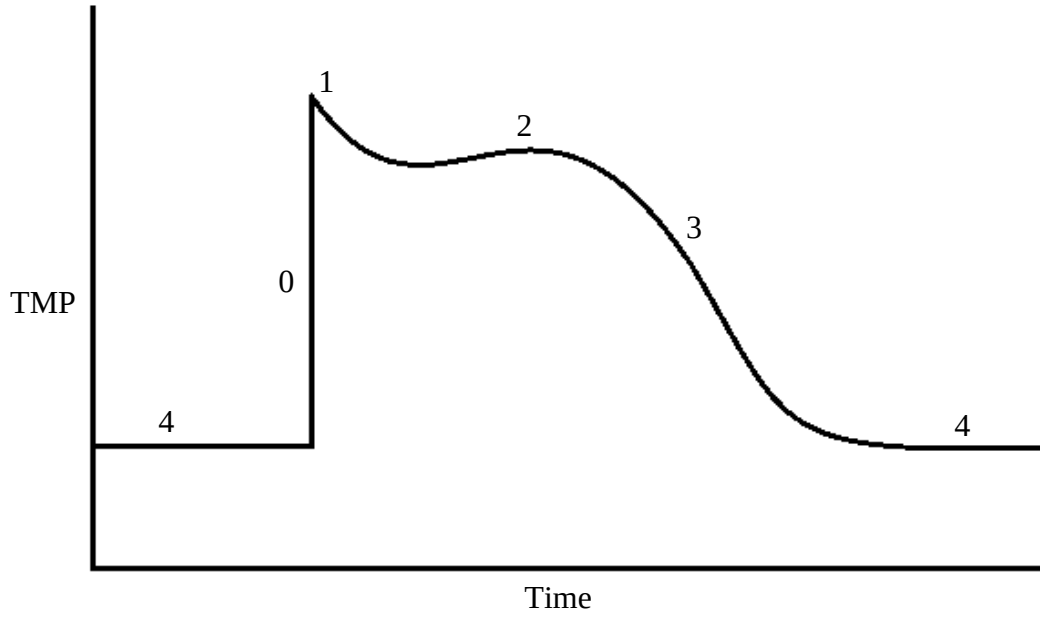

Figure 2.1 Cardiac Action Potential. The numbers on the figure 0-4 represent when each phase occurs in the AP. 0 is for the depolarization phase; 1 is for the early repolarization phase; 2 is for the plateau phase; 3 is for the repolarization phase; and 4 is for the resting phase.

Phase 4, referred to as the resting phase, is when the cardiac myocyte's TMP remains steady at around -90mV. This potential is controlled by the permeability of the cell membrane to different ions, with the steady outward leak of K^+ having the greatest effect. When an AP begins, phase 0 starts. Also known as the depolarization phase, phase 0 is when the TMP rapidly increases. This is typically caused by the adjacent cells electrically stimulating the cell through gap junctions. This triggers fast-type Na^+ channels to open, causing a rapid influx of positive Na^+ ions, with the TMP peaking around +25mV. Next in phase 1, referred to as early repolarization phase, is when the Na^+ channels deactivate and the transient K^+ channels open allowing K^+ ions to leave the cell which brings the TMP back near 0mV. Then phase 2, described as the plateau phase, starts. Here is when Ca^{2+} enters the cell through long-type Ca^{2+} channels, which electrically balances out the efflux of K^+ ions. This causes a plateau to form. Phase 3, known as the repolarization phase, is when more Ca^{2+} channels close and the steady outward flow of K^+ slowly lowers the potential back to resting potential.

2.3 Electrocardiogram

An ECG is a surface measurement of the electrical activity of the heart. It is often used to detect cardiac abnormalities such as arrhythmias, myocardial infarction, and electrolyte imbalances. With each phase of the cardiac cycle, the electrical signals within the heart affect the electrical signal on the surface of the body. The three main events of each heartbeat correspond to the three main features of the ECG. The P-wave corresponds to atrial depolarization, the QRS complex corresponds to the ventricular depolarization, and the T-Wave corresponds to ventricular repolarization.

2.4 Repolarization Alternans

Repolarization alternans is defined as the beat-to-beat variation in APD and has been linked to ventricular fibrillation [7-9]. This phenomenon can be detected in an ECG as alternans in the morphology and/or amplitude of the T-Wave [10, 11].

2.5 Depolarization Alternans

Alternans are not only found in the repolarization phase of APs, but are also found in the depolarization phase [12, 13]. A study published in our laboratory in 2012 looked at the relationship between APD alternans and $|dv/dt|_{max}$ alternans [6]. They found that when APD alternans were detected, $|dv/dt|_{max}$ alternans were also always detected. Most of the time (96%-Swine, 74%-Canine) these two were in-phase with each other. However, some of the time they were not. They concluded that these two alternans can become independent of each other. The following figure shows the possible relationships between APD and $|dv/dt|_{max}$ alternans.

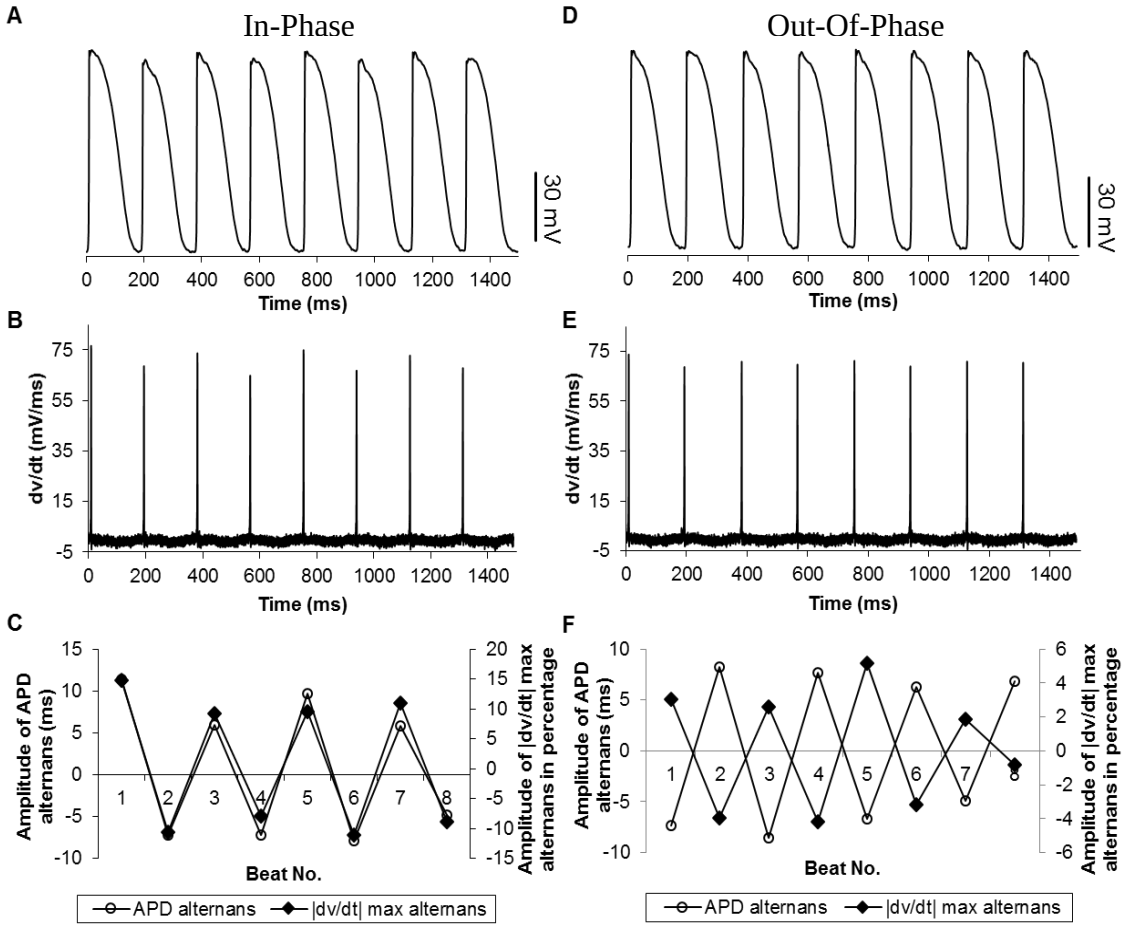

Figure 2.2 APD and $|dv/dt|_{max}$ In-Phase and Out-of-Phase relationship. Both APD (A, D) and $|dv/dt|_{max}$ (B, E) traces display beat-to-beat alternating patterns. (C, F) Show overlays of APD alternans (open circle) and alternans of $|dv/dt|_{max}$ (closed diamonds). (Reproduced with permission from [6])

2.6 Discordant Alternans

Spatial discord of alternans is a phenomenon where short (long) activation of the short-long sequence becomes long (short) as it travels spatially and has been linked to the onset of arrhythmia [14]. This discord can be affected by the phase between APD and $|dv/dt|_{max}$ alternans. One study used a canine ventricular myocyte model to show that by only changing the phase relationship between APD and $|dv/dt|_{max}$ alternans, discordance presence was affected [6]. When the two alternans were in-phase with each other, discordances among the cell occurred. However, when only the phase changed, discordance did not occur. This indicated that the phase might affect the occurrence of discordance.

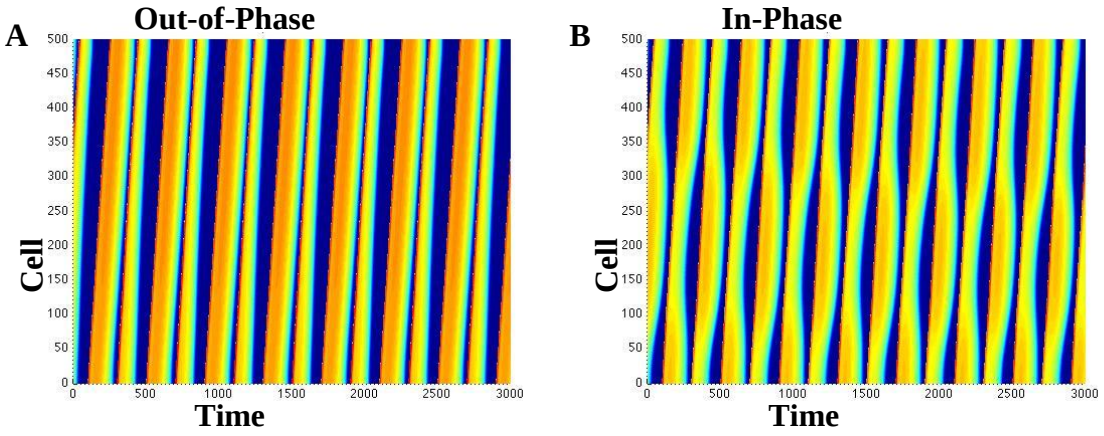

Figure 2.3 APD and $|dv/dt|_{max}$ In-Phase and Out-of-Phase Time-Space Plots. Time-Space plots of simulated Out-of-Phase (A) and In-Phase (B) relationship between depolarization and repolarization alternans. (Reproduced with permission from [6])

2.7 Alternans in ECG

Since it is not possible to measure $|dv/dt|_{max}$ from the ECG, a dipole field potential spatial model (described in the next section) created by Dr. Siqi Wang may provide a way to detect the effects of $|dv/dt|_{max}$ alternans from surface ECGs. To test this idea, a simulation was conducted using the model where every element in the model had the same $|dv/dt|_{max}$ alternans. The difference in $|dv/dt|_{max}$ between the beats showed up in the amplitude of the R-wave. The fallowing figure shows the difference between two beats with $|dv/dt|_{max}$ alternans in red at the peaks of the R-Wave.

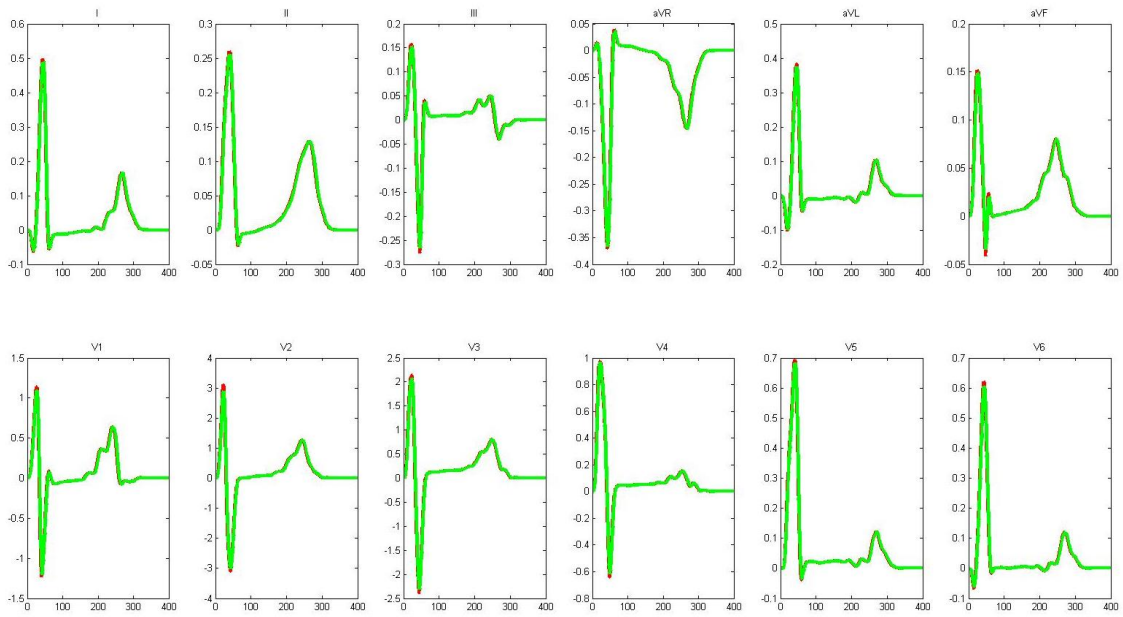

Figure 2.4 12 Lead ECG Model Showing Depolarization Alternans. Each tracing contains two beats from an ECG signal generated from AP with depolarization alternans. The red shows the difference between the two beats (Results provided by Dr. Siqi Wang).

2.8 Dipole Field Potential Spatial Model.

The dipole field potentials spatial model was used to look at the effects that different AP can cause on a standard surface ECG. This model was made up of 129,826 time-varying current dipole elements in the shape of a cone comparable in size to adult's ventricles. Each element had electrical properties that matched clinical and experimental data. For the torso, a homogenous volume conductor was used which matched the conduction properties and size of an adult human torso. The simulated ECG electrodes were positioned approximately the same distance and position of a traditional ECG's electrodes. Using the standard clinical lead locations, RA, LA, LL, V1, V2, V3, V4, and V5 were the lead locations used to compute ECGs.

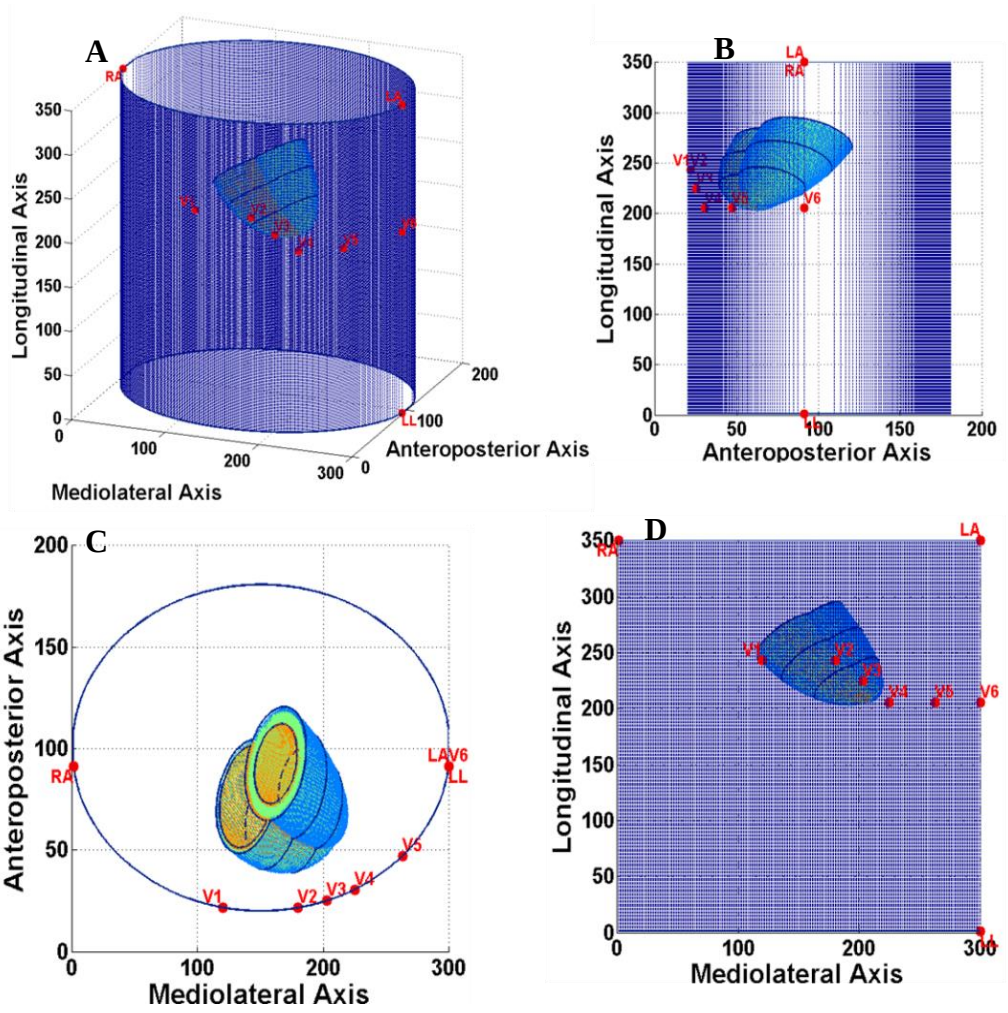

Figure 2.5 Dipole Field Potential Spatial Model. This figure shows a 3D view (**A**), front view (**B**) top view (**C**) and side view (**D**) of the model. The red dot represents the location of the different leads that would typically be used in an ECG. (Results provided by Dr. Siqi Wang).

In order to calculate the potential at the location for each ECG lead, first the model had to calculate the electrical field around each element. This was done by combining the intracellular potential, extracellular potential, and net membrane current per unit volume for each dipole element. Then integrating all those elements by knowing distance and direction for each ECG electrode, the body surface potential could be calculated.

To save computing time, the action potentials were generated and saved in look up tables that each element could pull from. The following figure compares a recorded intracellular AP and the modeled intracellular AP.

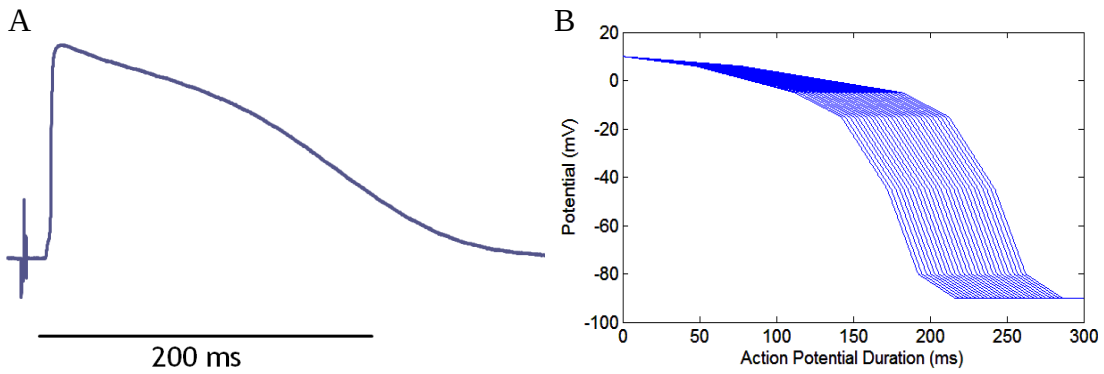

Figure 2.6 Actual AP vs Model AP. Shows a recorded intracellular human AP from our lab (**A**) vs a model Intracellular AP (**B**) (Results provided by Dr. Siqi Wang).

Chapter 3 Methods

For this study, 2 programs were created in MATLAB to detect alternans. The first program was used to detect TWA in the ECG. The second program looked at only the ECGs in which TWA were detected and analyzed RWA of the morphology and amplitude of the wave. Both programs used the same preprocessing and data reduction steps. Below is a flow chart of the process.

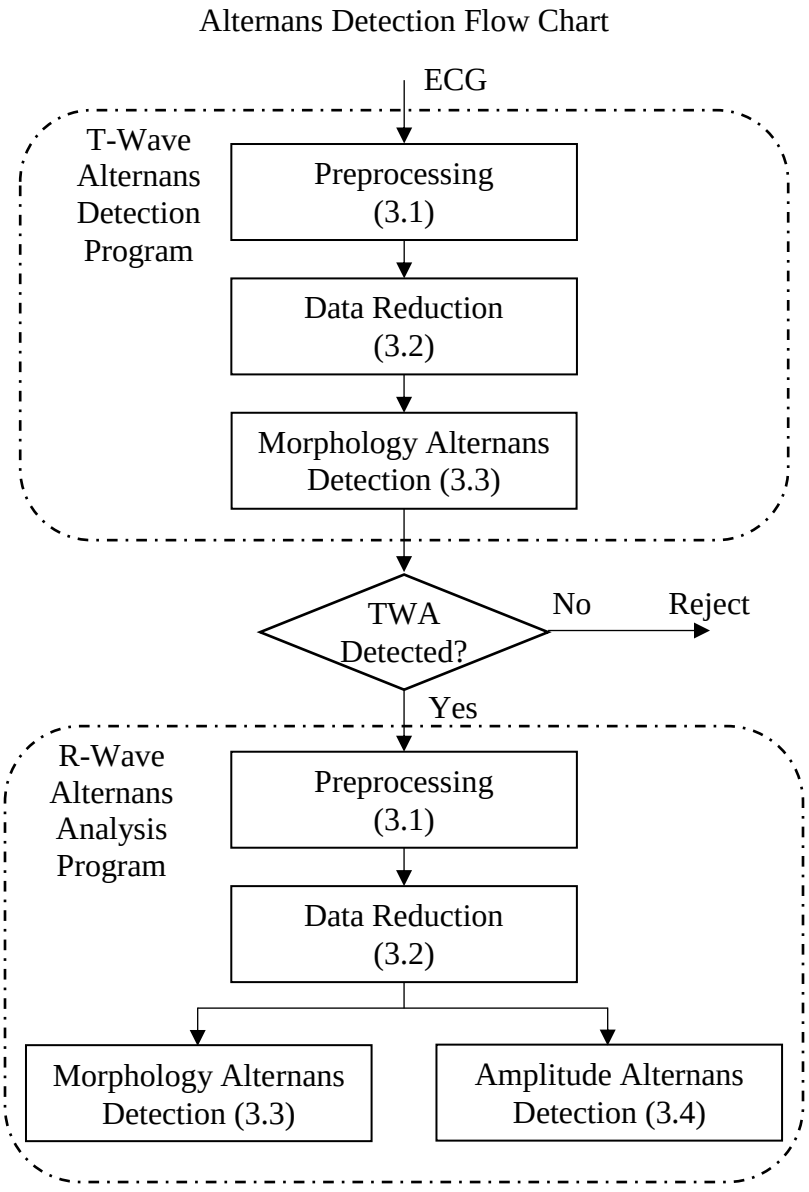

Figure 3.1 Alternans Detection Flow Chart.

3.1 Preprocessing

The first step of the preprocessing stage was to extract the ECG signal and sampling rate from the containing file. Then a zero-phase band pass digital filter was applied to the signal to remove excess noise. The filter was a second order Butterworth filter with cut off frequencies at 0.01 Hz and 60 Hz.

After the signal was filtered, each R-Wave peak was detected using the algorithm laid out by Pan and Tomkins QRS detection algorithm [15]. To accomplish this, the program first normalized the filtered ECG. For each sample in the signal, the signal's mean was subtracted and then divided by the signal's absolute max. A second order bandpass filter was then applied to the normalized signal with cut off frequencies of 5 Hz and 12 Hz. A five-point derivative then differentiated the filtered signal and each sample was then squared. Next, the signal was integrated by using a moving square window of 150ms, which is the approximate width of a QRS complex. Each R-wave peak was then located using the signal's mean as a threshold and minimum of 200ms between each peak.

After each R-wave peak had been located, fiducial points for each beat were located using the methods laid out by Weiss et. al. [11]. First, the T-wave preliminary boundaries were located by using the R-to-R (RR) interval between the current and previous R-wave peaks. If the RR interval was greater than 770ms, the T-wave was considered to start at 100ms after the R-peak. If the RR interval was between 770ms and 320ms, the T-wave was considered to start 40ms plus 7.8% of the RR interval and the R-peak. If the RR interval was less than 320ms, the T-wave was considered to start 65ms after the R-peak. The T-wave was considered to end 500ms after the R-peak if the RR interval was greater than 77ms or 65% of the interval after the R-peak if the RR interval was less than 77ms. The preliminary QRS complex start boundary was considered to start 50ms before the R-wave peak. The preliminary QRS complex end boundary was considered to end by either 80ms after the R-wave peak or the T-wave start boundary, whichever one was shortest. Then the final boundaries were located by first removing the linear baseline from each wave's window, by subtracting the window's mean from each sample. After squaring each sample, the cumulative summation of each sample was found. The final wave boundaries were located at 1% and 99% of the summation.

After the fiducial points were located, the baseline wander was removed from the original filtered signals. This was done by using a cubic spline interpolation. The control points used for this interpolation were the QRS start boundary for each beat.

3.2 Data Reduction

In the data reduction section, all abnormal beats were detected and labeled using both the RR interval and R-wave correlation laid out by Weiss et. al. [11]. If either method flagged a beat as abnormal, then it was considered abnormal.

The RR interval method flagged abnormal beats by taking the previous RR interval and comparing it to the mean of the preceding 7 RR intervals. If the previous RR interval was less than 90% of the mean, then the current, next, and previous beats were labeled abnormal.

The R-wave correlation method compared the current beat's R-wave to a median R-wave template generated from 127 beats. This was done by first normalizing each R-wave used in the template and the current R-wave. A 80ms window centered at each R-wave peak was used as the window for the wave. Then the mean of the isoelectric segment, defined as 10ms before the start of each QRS complex, was subtracted from each sample to normalize each R-wave window. Then a median R-wave template was generated from the 127 normalized beats. Next, the current R-wave's window and the median R-wave's template were cross-correlated twice to insure proper alignment. After that, the correlation coefficient was calculated between the beats. If the coefficient was less than 95%, then the tested beat was considered abnormal.

3.3 Morphology Alternans Detection

To quantify alternans in the morphology of an ECG, the spectral method laid out by Weiss et al was used [11]. This was done on a beat-by-beat basis by analyzing 128 beat sequence, then shifting the sequence one beat to the right. This was repeated until all the beats in the ECG were part of a sequence.

First, the beat sequence was tested to see if it was indeterminate. To do this, the number of normal beats was compared to the total number of beats. If there are less than 90% normal beats within the sequence, then that sequence was labeled indeterminate.

The next step was to generate a cumulative power spectrum of the 128 beats in the sequence. This was done by first generating an even and an odd median template from the normal beats. Next, an array was created from all the beats. The rows contained the beats and the columns were the samples. If the beat was abnormal, a corresponding even or odd template replaced the row. Then, a Fast Fourier Transform (FFT) was calculated on each column and the rows were summed up to generate a cumulative power spectrum.

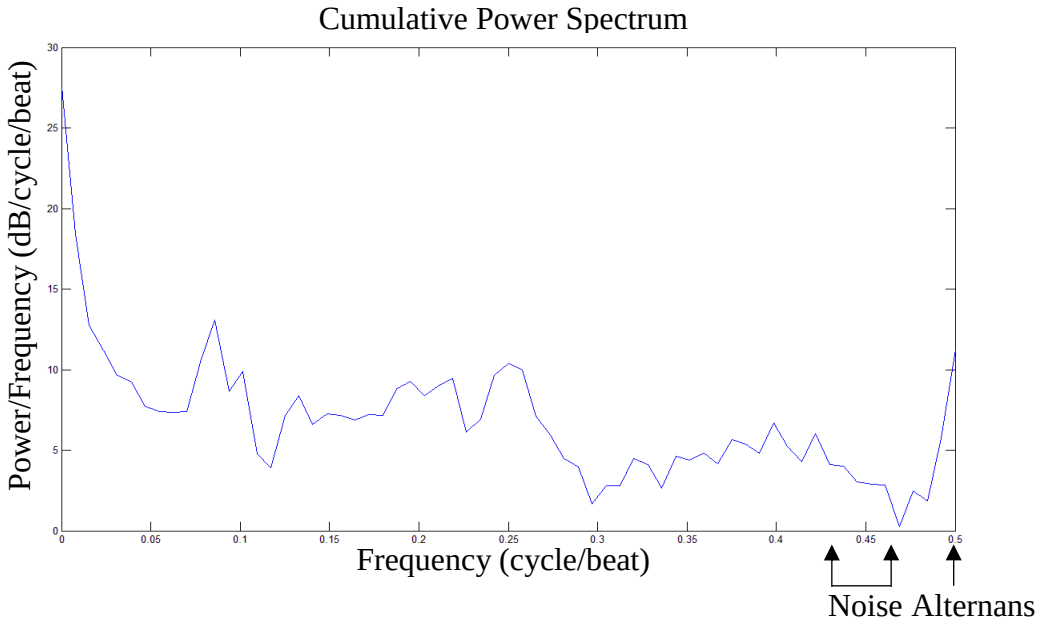

Figure 3.2 Cumulative Power Spectrum. Alternans occur at the 0.5 cycle/beat and noise was between 0.43 and 0.46 cycles/beat. (Signal from Physionet.org [16])

This cumulative power spectrum was used to determine if the series of beats contained alternans. The following equations were used.

$$alternans\ voltage\ (\mu V) = \sqrt{alternans\ peak - \mu_{noise}}$$

Equation 3.1 Alternans Voltage Equation. The $alternans\ peak$ was located at 0.5 cycle/beat and $\mu_{noise}$is the mean of the noise window between 0.43 and 0.46 of the aggregated power spectrum.

$$K_{score} = (alternans\ peak - \mu_{noise})/\sigma_{noise}$$

Equation 3.2 Alternans K_{score} Equation. The $alternans\ peak$ was located at 0.5 cycle/beat and $\mu_{noise}$is the mean and σ_{noise} was the standard deviation of the noise window between 0.43 and 0.46 of the aggregated power spectrum.

The alternans voltage equation directly measures the magnitude of alternans within the series. The K_{score} was the statistical significance of the alternans voltage. To determine if alternans were present, the following criteria needed to be met: (1) alternans voltage $\geq$ 1.0 μV and $K_{score} \geq 3$ [11].

The fiducial points located in the preprocessing defined the window for each wave. For the T-wave, the window was from the end of the QRS complex to the end of the T-wave. For the R-wave, the window was 80ms centered at the peak of the R-wave.

3.4 R wave Amplitude Alternans Detection

In this study, to classify a series of beats as containing R wave amplitude alternans, three criteria needed to be met. First, the peak height needed to alternate from beat to beat (i.e. tall-short-tall or short-tall-short) for 5 times or more, i.e. five sequential alternating changes in height. Second, the absolute difference between each beat's amplitude and the previous must be greater than 5% of the mean of all the R-wave peak heights in the signal. Third, none of the beats in the series were labeled abnormal.

3.5 Validation of TWA computation

To ensure the TWA detection program was working properly, the program was validated using the challenge data and results from PhysioNet's 2008 T-Wave Alternans Challenge [17]. This challenge asked participants to create an automated system that could rank 100 two minute segments of ECG signals by the magnitude of T-Wave alternans from 1 to

100. Their rankings would then be compared to a reference ranking and scored. There were 56 human ECGs obtained from individuals at risk for SCD, 12 from healthy subjects and 6 from a normal sinus rhythm database. The other 32 ECGs were synthetic with known TWA magnitude. The reference ranking was determined from the median participant's rankings who could successfully distinguish between the high and low synthetic ECGs. Because PhysioNet's challenge was over before the study started, we could compare the final reference ranking to our program's ranking. The following chart shows the reference ranking vs the program's ranking.

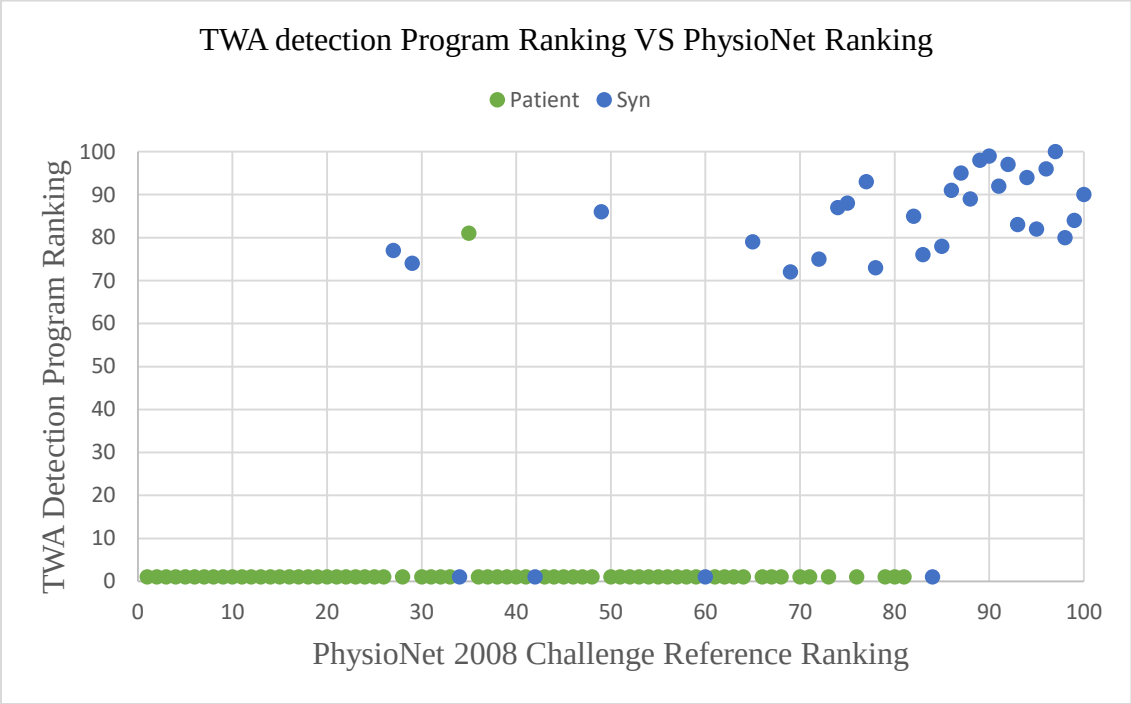

Figure 3.3 Graph PhysioNet challenge rankings vs the programs rankings. The X-axis is the reference ranking of each file in the challenge with 1 being the least TWA detected, and 100 being the most detected. The Y-axis is how our program ranked the files, with 1 being the least TWA detected and 100 being the most. The blue dots are synthetically generated ECG samples that have known TWA magnitudes. The Green dots are samples from various human ECG's in the PhysioNet Library.

3.6 Statistical analysis of sequential changes in heights of R wave

For this part of the study, the purpose was to determine the probability that a series of sign changes could have happened by chance. We chose an empirical method to determine the probability. To do this we first generated a sequence of 10,000 random binary numbers with equal probability of being 1 or 0. We then looked for how many times there were 5 number changes (i.e. 101010 or 010101). Then we calculated the probability by taking that number and dividing it by the number of samples tested. After repeating this 10,000 times and taking the average probability, we obtained that the probability that a sequence of 5 changes could occur is 3.1%, i.e. comparable to a P-value < 0.05.

Chapter 4 Data and Results

4.1 Data Source

The data used in this study came from 9 different databases on PhysioNet.org [16]. PhysioNet's website contains a large number of recorded human physiological signals that are freely available to the public under the ODC Public Domain Dedication and License v1.0 to be used for research. The National Institute of General Medical Science (NIGMS) and the National Institute of Biomedical Imaging and Bioengineering (NIBIB) supports this website. A description of each database used is in the following paragraphs.

The European ST-T database (EDB) was assembled from subjects who were diagnosed or suspected to have myocardial ischemia and had ST and T-wave changes [16, 18]. There were 90 ECG recordings from 79 different subjects, each 2 hours long. Each recording was sampled at 250 Hz with 12-bit resolution over a 20mV input range.

The Long-Term AF Database (LTAFDB) was assembled from subjects with paroxysmal or sustained atrial fibrillation [16, 19]. There were 84 long-term ECG recordings with lengths ranging from 24 to 25 hours. Each recording was sampled at 128 Hz with 12-bit resolution over 20 mV range.

The MIT-BIH Long Term Database (LTDB) contains 7 long-term ECG recordings from 14 to 22 hours [16]. Each record sampled at 250 Hz with 12-bit resolution over a 20mV range.

The Long-Term ST Database (LTSTDB) was assembled from subjects that exhibit a variety of events in the ST segment portion [16, 20]. These include ischemic ST episodes, axis-related non-ischemic ST episodes, episodes of slow ST level drive, or a mixture of all 3. There were 86 ECG recordings from 80 subjects each ranging from 21 to 24 hours long. Each record was sampled at 250 Hz with 12-bit resolution of a ±10 mV range.

The MIT-BIT arrhythmia database (MITDB) was comprised of ECG recordings that were used in the study of cardiac arrhythmias [16, 21]. There were 48 ECG recordings from 47 subjects each having a length of 30 minutes. Each recording was digitized at 360 Hz with 11-bit resolution over a 10mV range.

The Sudden Cardiac Death Holter Database (SDDB) was made up from complete holster recordings from patients that had a sustained ventricular tachyarrhythmia with most having had actual cardiac arrest [16, 22]. There are 23 complete holter recordings, which include 18 subjects with underlying sinus rhythm, 1 who was continuously paced, and 4 with atrial fibrillation. All patients had a sustained ventricular tachyarrhythmia, while most had experienced cardiac arrest. Each recording was recorded at 250 Hz with 12-bit resolution over a 20mV range.

The MIT-BIH ST Change Database (STDB) contained ECGs recordings that exhibit ST segment abnormalities [16, 23]. There are 28 recordings, with 23 of them recorded during an exercise stress test and showed transient ST depression. The other 5 recordings were excerpts from long-term ECG recordings that exhibit ST elevation. Each recording was sampled at 360 Hz with 12-bit resolution over 20mV range.

The St.-Petersburg Institute of Cardiological Technics 12-lead arrhythmia database (INCARDTDB) contained ECGs from patients being tested for coronary artery disease [16]. It was comprised of 75 half-hour recordings from 32 holter recordings. None of the patients had pacemakers, while most of them had ventricular ectopic beats and displayed signs of ischemia, coronary artery disease, conduction abnormalities and arrhythmias. Each recording was sampled at 257 Hz with gains varying from 250 to 1100 analog-to-digital converter units per millivolt.

4.2 Alternans Detection

This study analyzed 441 ECGs that came from 8 different databases from PhysioNet.org. Of those 441 ECG, TWA was detected in 318 of them. Of the 318 files that TWA was detected, morphological RWA was detected in 309 and amplitude RWA was detected in 287.

Table 4.1 Number of Files in which Alternans Were Detected. This table shows how many files from each database were analyzed and TWA was detected. It also shows the percentage of files that RWA morphological and amplitude alternans were detected from the files TWA were detected.

Database	Total # of ECG	# of ECG that TWA was Detected	% of TWA ECG that Morphological RWA was Detected	% of TWA ECG that Amplitude RWA was Detected
edb	90	84	100%	90.4%
ltafdb	84	41	100%	100%
ltdb	7	6	83.3%	83.3%
ltstdb	86	65	100%	100%
mitdb	48	33	90.9%	72.7%
sddb	23	21	100%	100%
stdb	28	23	95.7%	78.3%
incartdb	75	45	91.1%	82.2%
All ECG's	**441**	**318**	**97.2%**	**90.3%**

4.3 Morphological RWA

After TWA was detected in each ECG, the next step was to look for alternans in the morphology of the R-wave. The program looks at 128 beat sequences and flags them positive if alternans was found or negative if not, based on the description in chapter 3. Then the number of positive sequences was divided by the number of positive and negative sequences to find the percentage of positive morphological RWA sequences within in the ECG. The table below shows the average and standard deviation of the percentages of positive sequences from all the files in each database. In addition, it shows the percentage from the ECG that had the highest positive percentage within that database.

Table 4.2 Morphological RWA. The percentage of positive morphological RWA was calculated by finding the percentage of positively flagged alternans sequences of the total of all positive and negative flagged alternans sequences.

Database	% of Positive Morphology RWA (Avg±Std)	% of Positive Morphology RWA (Max)
edb	3.20% ± 1.90%	12.90%
ltafdb	6.36% ± 3.08%	18.79%
ltdb	8.76% ± 1.84%	10.94%
ltstdb	3.28% ± 1.40%	9.16%
mitdb	5.93% ± 9.08%	46.32%
sddb	4.19% ± 2.20%	9.72%
stdb	3.71% ± 4.54%	20.36%
incartdb	6.12% ± 7.52%	44.23%
All ECG's	**4.48% ± 4.65%**	**46.32%**

4.3 Amplitude RWA

The second part of this project was to look for amplitude RWA. Here we looked for a series of 6 normal beats or more, the height of these beats to alternate and if the absolute change from peak to peak was greater than 5% of the mean of all the peaks. Table 4.3 shows the average, standard deviation, and max percentage of beats that are part of one of these sequences for each database. Table 4.4 shows the duration of each sequence.

Table 4.3 Amplitude RWA Number of Beats. Percentage of beats that are part of a RWA sequence.

Database	% of Beats part of an amplitude RWA sequence (Avg±Std)	% of Beats part of an amplitude RWA sequence (Max)
edb	3.23% ± 3.25%	13.33%
ltafdb	2.31% ± 2.58%	10.77%
ltdb	1.73% ± 1.88%	4.79%
ltstdb	3.32% ± 3.28%	10.14%
mitdb	5.76% ± 7.83%	38.27%
sddb	3.98% ± 5.11%	19.08%
stdb	2.96% ± 2.26%	9.15%
incartdb	2.75% ± 2.38%	10.02%
All ECG's	**3.28% ± 3.84%**	**38.27%**

Table 4.4 Amplitude RWA Durations. The duration was how many sign changes occur in a sequence.

Database	Mean Duration Length (Avg±Std)	Median Duration Length (Avg±Std)	Max Duration Length (Max)	Number of Durations (Avg±Std)
edb	5.69 ± 0.39	5.37 ± 0.54	20	39.08 ± 42.99
ltafdb	5.66 ± 0.29	5.21 ± 0.41	25	228.63 ± 296.09
ltdb	5.46 ± 0.31	5.14 ± 0.35	14	128.40 ± 118.49
ltstdb	5.83 ± 0.60	5.36 ± 0.53	133	492.74 ± 509.48
mitdb	5.74 ± 0.62	5.44 ± 0.52	15	15.54 ± 19.83
sddb	5.95 ± 0.54	5.37 ± 0.65	32	221.57 ± 236.59
stdb	5.82 ± 0.51	5.36 ± 0.52	21	11.00 ± 8.56
incartdb	5.78 ± 0.93	5.34 ± 0.53	19	7.59 ± 7.32
All ECG's	**5.76 ± 0.56**	**5.33 ± 0.52**	**133**	**176.02 ± 333.02**

Chapter 5 Discussion

Researchers have studied TWA as a predictor for SCD [1, 4]. With its very strong negative predictive value, it is a very appealing test that could potentially weed out patients who are not at risk for SCD. However, with its weak PPV, it can cause people who are falsely flagged for SCD to waste time and money on treatment that they do not need. The overall goal of our laboratory is to investigate potentially complementary tests in order to improve the PPV of the TWA test. One potential feature of electrical function that has shown promise in recent years was alternans in the depolarization phase of APs and its relationship with alternans of APD.

Using mathematical models and tissue level microelectrode recordings, the relationship between $|dv/dt|_{max}$ alternans and APD alternans affects if discordant alternans can occur in tissue [12, 24]. Until now, $|dv/dt|_{max}$ alternans have only been detected using microelectrodes. However, using a dipole field potential spatial model, the effect of $|dv/dt|_{max}$ alternans may be detectible in the R-wave of ECGs.

The purpose of this study was to determine if alternans of the R-wave amplitude and morphology are detectable in clinical grade ECGs.

5.1 TWA Detection Program

For this project, the purpose was to determine if RWA occurs in ECGs that already have TWA. We decided to use the spectral method to detect TWA because it was well established as a detector of TWA [11].

To verify that our TWA detection program was accurate, we used the 2008 PhysioNet's TWA challenge as our testing standard. We had our program rank the dataset provided in the challenge and compared our results to its final rankings. Figure 3.4 shows that even through our program did not detect TWA in every ECG from the PhysioNet's challenge, the ECGs that it did detect, were among the highest rankings. Also, the program validated well with synthetic ECGs (with known TWA) than the clinical ECGs with unknown TWA. This indicates that our program had a conservative, but accurate approach when detecting TWA.

The program was conservative because each ECG from the PhyioNet's challenge was 2 minutes long. Our program looked at sequences that are 128 beats long, which was often longer than half the total ECG length. If the signal was noisy and not enough beats were normal in the ECG, all of the sequences were labeled indeterminate. This would cause the program to say there was no TWA present in the ECG. Because the objective at this stage was not looking at the frequency of occurrence of RWA, but looking for its presence, the conservative nature of the program was not a major concern.

5.2 Morphological RWA

For this study, we used a method similar to that used for TWA detection to determine if alternans in the morphology of the R-wave does occur. When looking for morphological RWA, we used the same logic used to locate TWA, because this method was already shown to detect alternans of the T wave.

Table 4.1 shows that of the 318 files in which TWA was detected, 309 of those files contained morphological RWA. We can also see that within the ECG, morphological RWA was present on average in 5% of the signal (table 4.2), although it can reach as high as 46%. This indicates that not only does morphological RWA occur in ECGs when TWA was detected, it could be a common occurrence. Further research is required to better estimate the frequency of occurrence of this phenomenon.

5.3 Amplitude RWA

The dipole field potentials spatial model that Dr. Siqi Wang developed showed that $|dv/dt|_{max}$ alternans appeared as alternans in the amplitude of the R-wave. For this study, we wanted to see if the amplitude of the R-wave had alternans when TWA was present.

We discovered that the average percentage of beats that were part of an amplitude RWA sequence was 3.2%. We also saw this percentage to be as high as 38.27%. These results supports the possibility of using RWA as a means to look at the relationship between depolarization alternans and TWA.

In table 4.4, we see that the average length of the amplitude RWA duration was around 5.7, which was just slightly larger than the minimum length for a sequence. But we did see duration lengths as long as 133 beats. This leads us to conclude that we can potentially use the relationship between amplitude RWA and TWA, to look at the relationship of the depolarization and repolarization phase of AP alternans.

5.3 Conclusion

In Conclusion, this study determined that in clinical grade ECGs, where TWA can be detected, RWA was detectable. This observation supports further exploration of whether the RWA has the potential be used as a complementary test to TWA for prediction of SCD. This use has the potential to improve the PPV of the TWA. Improving the PPV value will greatly reduce unnecessary treatment and excessive spending for SCD.

References

[1] D. P. Zipes and H. J. Wellens, "Sudden cardiac death," *Circulation,* vol. 98, pp. 2334-51, Nov 24 1998.

[2] A. S. Go, D. Mozaffarian, V. L. Roger, E. J. Benjamin, J. D. Berry, M. J. Blaha, *et al.*, "Heart disease and stroke statistics--2014 update: a report from the American Heart Association," *Circulation,* vol. 129, pp. e28-e292, Jan 21 2014.

[3] R. Deo and C. M. Albert, "Epidemiology and genetics of sudden cardiac death," *Circulation,* vol. 125, pp. 620-37, Jan 31 2012.

[4] A. A. Armoundas, G. F. Tomaselli, and H. D. Esperer, "Pathophysiological basis and clinical application of T-wave alternans," *J Am Coll Cardiol,* vol. 40, pp. 207-17, Jul 17 2002.

[5] A. K. Gehi, R. H. Stein, L. D. Metz, and J. A. Gomes, "Microvolt T-wave alternans for the risk stratification of ventricular tachyarrhythmic events: a meta-analysis," *J Am Coll Cardiol,* vol. 46, pp. 75-82, Jul 5 2005.

[6] L. Jing, A. Agarwal, S. Chourasia, and A. Patwardhan, "Phase Relationship between Alternans of Early and Late Phases of Ventricular Action Potentials," *Front Physiol,* vol. 3, p. 190, 2012.

[7] M. L. Koller, M. L. Riccio, and R. F. Gilmour, Jr., "Dynamic restitution of action potential duration during electrical alternans and ventricular fibrillation," *Am J Physiol,* vol. 275, pp. H1635-42, Nov 1998.

[8] J. J. Fox, J. L. McHarg, and R. F. Gilmour, Jr., "Ionic mechanism of electrical alternans," *Am J Physiol Heart Circ Physiol,* vol. 282, pp. H516-30, Feb 2002.

[9] I. Banville, N. Chattipakorn, and R. A. Gray, "Restitution dynamics during pacing and arrhythmias in isolated pig hearts," *J Cardiovasc Electrophysiol,* vol. 15, pp. 455-63, Apr 2004.

[10] R. L. Verrier, T. Klingenheben, M. Malik, N. El-Sherif, D. V. Exner, S. H. Hohnloser, *et al.*, "Microvolt T-wave alternans physiological basis, methods of measurement, and clinical utility--consensus guideline by International Society for Holter and Noninvasive Electrocardiology," *J Am Coll Cardiol,* vol. 58, pp. 1309-24, Sep 20 2011.

[11] E. H. Weiss, F. M. Merchant, A. d'Avila, L. Foley, V. Y. Reddy, J. P. Singh, *et al.*, "A novel lead configuration for optimal spatio-temporal detection of intracardiac repolarization alternans," *Circ Arrhythm Electrophysiol,* vol. 4, pp. 407-17, Jun 2011.

[12] H. S. Karagueuzian, S. S. Khan, K. Hong, Y. Kobayashi, T. Denton, W. J. Mandel, *et al.*, "Action potential alternans and irregular dynamics in quinidine-intoxicated ventricular muscle cells. Implications for ventricular proarrhythmia," *Circulation,* vol. 87, pp. 1661-72, May 1993.

[13] S. M. Narayan, J. D. Bayer, G. Lalani, and N. A. Trayanova, "Action potential dynamics explain arrhythmic vulnerability in human heart failure: a clinical and modeling study implicating abnormal calcium handling," *J Am Coll Cardiol,* vol. 52, pp. 1782-92, Nov 25 2008.

[14] Z. Qu, A. Garfinkel, P. S. Chen, and J. N. Weiss, "Mechanisms of discordant alternans and induction of reentry in simulated cardiac tissue," *Circulation,* vol. 102, pp. 1664-70, Oct 3 2000.

[15] J. Pan and W. J. Tompkins, "A real-time QRS detection algorithm," *IEEE Trans Biomed Eng,* vol. 32, pp. 230-6, Mar 1985.
[16] A. L. Goldberger, L. A. Amaral, L. Glass, J. M. Hausdorff, P. C. Ivanov, R. G. Mark, *et al.*, "PhysioBank, PhysioToolkit, and PhysioNet: components of a new research resource for complex physiologic signals," *Circulation,* vol. 101, pp. E215-20, Jun 13 2000.
[17] G. Moody, "The PhysioNet / Computers in Cardiology Challenge 2008: T-Wave Alternans," *Comput Cardiol,* vol. 2008, pp. 505-508, 2008.
[18] D. Gordon, A. H. Kadish, D. Koolish, T. Taneja, J. Ulphani, J. J. Goldberger, *et al.*, "High-resolution electrical mapping of depolarization and repolarization alternans in an ischemic dog model," *Am J Physiol Heart Circ Physiol,* vol. 298, pp. H352-9, Feb 2010.
[19] S. Petrutiu, A. V. Sahakian, and S. Swiryn, "Abrupt changes in fibrillatory wave characteristics at the termination of paroxysmal atrial fibrillation in humans," *Europace,* vol. 9, pp. 466-70, Jul 2007.
[20] F. Jager, A. Taddei, G. B. Moody, M. Emdin, G. Antolic, R. Dorn, *et al.*, "Long-term ST database: a reference for the development and evaluation of automated ischaemia detectors and for the study of the dynamics of myocardial ischaemia," *Med Biol Eng Comput,* vol. 41, pp. 172-82, Mar 2003.
[21] G. B. Moody and R. G. Mark, "The impact of the MIT-BIH arrhythmia database," *IEEE Eng Med Biol Mag,* vol. 20, pp. 45-50, May-Jun 2001.
[22] S. D. Greenwald, "The development and analysis of a ventricular fibrillation detector," M s, Massachusetts Institute of Technology, 1986.
[23] P. Albrecht, "ST segment characterization for long term automated ECG analysis," M s, Massachusetts Institute of Technology, 1983.
[24] L. Jing, A. Agarwal, and A. Patwardhan, "Supernormal Conduction and Suppression of Spatially Discordant Alternans of Cardiac Action Potentials," *Front Physiol,* vol. 6, p. 407, 2015.

Vita

Author's Name:
David Ray Wasemiller

Education:
B.S. in Engineering, Electrical and Computer Emphasis: May 2008
Andrews University, Berrien Springs, MI 2008

Profession:
Senior Electrical Controls Engineer: February 2014 – August 2014
Electrical Controls Engineer: July 2011 – February 2014
Shick USA, Kansas City, MO,

Systems Control Engineer, November 2008 – February 2010
Mac Equipment Inc., Sabetha, Kansas